Phase Transitions in Isolated Vortex Chains

Matthew J. W. Dodgson
Theory of Condensed Matter Group, Cavendish Laboratory, Cambridge, CB3 0HE, UK.
(Dated: January 11, 2002)

In very anisotropic layered superconductors (e.g. $Bi_2Sr_2CaCu_2O_x$) a tilted magnetic field can penetrate as two co-existing lattices of vortices parallel and perpendicular to the layers. At low out-of-plane fields the perpendicular vortices form a set of isolated vortex chains, which have recently been observed in detail with scanning Hall-probe measurements. We present calculations that show a very delicate stability of this isolated-chain state. As the vortex density increases along the chain there is a first-order transition to a buckled chain, and then the chain will expel vortices in a continuous transition to a composite-chain state. At low densities there is an instability towards clustering, due to a long-range attraction between the vortices on the chain, and at very low densities it becomes energetically favorable to form a tilted chain, which may explain the sudden disappearance of vortices along the chains seen in recent experiments.

PACS numbers: 74.60.Ec, 74.60.Ge

I. INTRODUCTION

The vortex system in layered superconductors,[1] which includes the high-T_c cuprates, displays a rich set of physical phenomena, such as a thermodynamic melting transition,[2] a pinning-induced disordering transition,[3] and various structural transitions at different angles.[4,5] The average density and orientation of the vortices are controlled by the magnetic field, because each vortex carries one quantum of flux, $\Phi_0 = hc/2e$. In this paper we are concerned with the vortex chains that appear in a certain regime of tilted magnetic fields. These chains, which consist of a high density of flux lines perpendicular to the layers, were first observed with the Bitter decoration technique by Bolle et al.[6] A qualitative explanation followed shortly[7] in terms of the proposed crossing-lattice state in tilted fields.[8,9] This state consists of a lattice of flux lines perpendicular to the layers crossed by a lattice of flux lines along the layers. The in-plane lattice is strongly distorted due to the anisotropy,[10] and has a large spacing along the layers. Huse surmised that a possible attractive interaction between the two species of flux line would lead to a higher density of out-of-plane flux lines along chains, with an inter-chain separation equal to the in-plane flux-line spacing. This picture seems to be consistent with the experimental observations.[11] The energy of the crossing-lattice state was considered by Benkraouda and Ledvij,[12] who found a transition from a single lattice of tilted flux lines to the crossing-lattice state as the tilt angle is increased for sufficiently large anisotropy. Their work, however, neglected interactions between the two crossing lattices.

Interest in the crossing-lattice state has been revitalized in the last couple of years. Koshelev[13] has shown that the regime for crossing lattices is larger than previously expected. This is because a correct treatment must include the interactions between the perpendicular flux lines, and a distortion away from ideal crossing lattices has a lower energy. Experimental evidence comes in the form of the unusual dependence of the melting temperature of the vortex lattice as a function of magnetic field angle,[14,15] which is consistent with the crossing-lattice state rather than a single tilted flux-line lattice.[13] In addition, the work of Koshelev explained quantitatively the attraction of perpendicular flux lines that leads to the vortex-chain state in a certain field range. Apart from more detailed work on the melting transition,[4] and on magnetization curves,[5] these concepts have also inspired recent scanning Hall-probe measurements[16] on the vortex-chain state. These experiments are similar to the Bitter decoration technique in that they only probe the field distribution emanating from the surface of the superconductor. However, they have the advantage of speed and resolution, and are not a "one-off" measurement, so that the system can be finely tuned to observe different effects. These new experiments have shown unexpected properties within the chain state. In particular, it is possible to tune to a field range where all of the out-of-plane flux lines are arranged in chains. It is this "isolated-chain state" that we will study in this paper.

We will use the following geometry. The z-axis is perpendicular to the layers, and the component of magnetic induction B_z determines the density of "pancake" vortices[17] in every superconducting layer. The in-plane field is along the x-axis, and B_x gives the density of the flux lines in this direction. These in-plane flux lines have their centers in the spacing between layers, and so are commonly called Josephson vortices.[18] A z-directed flux line is made from a stack of pancake vortices, and contains circulating currents in the layers up to a distance of the penetration depth, $\lambda_{\rm ab} \equiv \lambda$, from the vortex center. A Josephson vortex in the x-direction has an ellipsoidal current pattern, with the flux and currents decaying over the much larger distance $\lambda_{\rm c} = \gamma\lambda$ in the y-direction. Here, γ is the anisotropy ratio, which is large for weakly coupled layers. The phase singularity of the Josephson vortex is confined between two neighboring layers, with separation d, where the phase difference across the layers changes by 2π over a distance of the Josephson length γd.

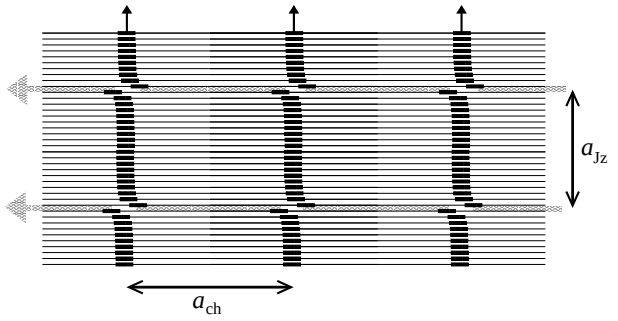

FIG. 1: Optimal displacements of the vortex chain of pancake stacks due to the crossing of Josephson vortices, using the parameters appropriate for BiSCCO quoted in the text. The figure takes the results from calculations for $a_{ch} = 10\lambda$, and $a_{Jz} = 20d$ which for the isolated-chain state corresponds to $B_x = 53$ G and $B_z = 0.8$ G. The displacements are magnified by two for clarity, and the z-scale is not the same as the x-scale.

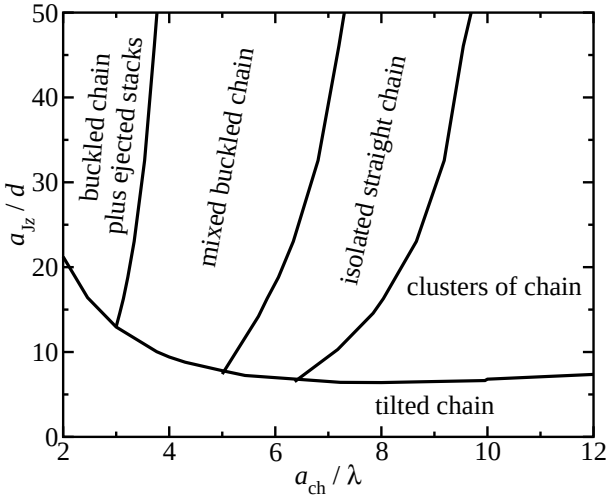

FIG. 2: Phase diagram of the isolated vortex chain, showing four phases: Isolated chain of tilted stacks; Isolated chain of straight stacks crossing Josephson vortices; Isolated buckled chain; state with chains plus ejected vortices. Axes show the spacing of pancake vortices a_{ch} and the Josephson vortex spacing a_{Jz} within the chain.

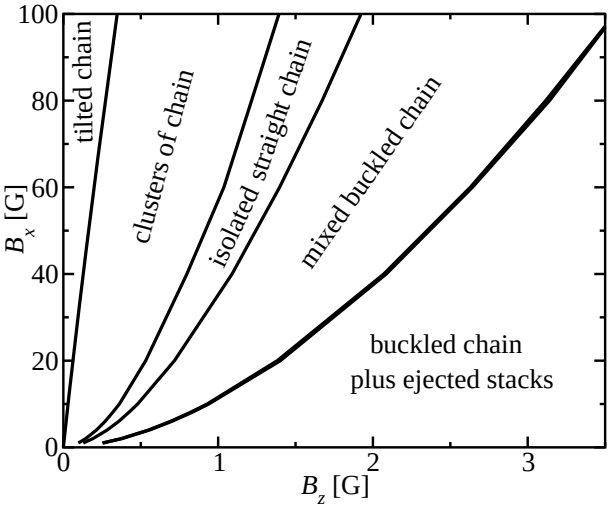

FIG. 3: Same phase diagram as in Fig. 2 but with axes converted to the the in-plane and out-of plane components of magnetic field, assuming the Josephson vortices form a regular stretched triangular lattice.

The most simple structure of the crossing-lattice state is when an ideal triangular lattice (with spacing $a_P = [(2/\sqrt{3})\Phi_0/B_z]^{1/2}$) of pancake-vortex stacks crosses a stretched triangular lattice of Josephson vortices, with separation in the z-direction of $a_{Jz} = [(2/\sqrt{3})\Phi_0/B_x]^{1/2}/\sqrt{\gamma}$. Koshelev has shown how the interactions between pancake stacks and Josephson vortices lead to an effective attraction.[13] At the low pancake densities we are interested in here ($B_z < \Phi_0/\lambda^2$) this means that there will be large distortions from the ideal triangular pancake-vortex lattice, with a higher density of pancake stacks located over the centers of the Josephson vortices. This leads to the high-density chains of pancake stacks that are observed by Bitter decoration,[6,11] with an inter-chain spacing of $a_{Jy} = \sqrt{\gamma}[(\sqrt{3}/2)\Phi_0/B_x]^{1/2}$. Eventually, for small $B_z \ll \Phi_0/\lambda^2$, all of the pancakes lie over the Josephson vortices. This isolated-chain state has a pancake-stack separation along the chains of $a_{ch} = (\Phi_0/B_z)/a_{Jy}$, see Fig. 1.

The crossing lattices must compete energetically with the more conventional tilted lattice of vortices. This is quite similar to the vortex lattice in a continuous superconductor, only there is a kinked structure along each vortex with a periodicity $L = d(B_x/B_z)$. The anisotropy of the currents mean that there is a stretched aspect ratio of this lattice. In addition, this distortion may be different from that expected from simple rescaling[19] due to the attraction of tilted vortices along the direction of tilt. This may lead to a "tilted chain state",[20] which is distinct from the crossing chains mentioned above. Koshelev showed that for intermediate pancake densities $B_z > \Phi_0/\lambda^2$ there should be a transition at a small value of $B_x = B_x^* \approx 0.01B_z$ between the tilted lattice ($B_x < B_x^*$) and the crossing lattices ($B_x^* < B_x$).

In this work we will concentrate on very small out-of-plane fields and $B_z \ll B_x < \Phi_0/\lambda^2$ when all of the pancake stacks become attached to the centers of the Josephson vortices, giving the isolated-chain state observed in recent scanning Hall probe measurements.[16] We find that the stability of the isolated-chain state is quite delicate. We first note in Section II that the existence of a stable crossing configuration in the isolated chains is only possible for large enough anisotropy, layer spacing, and pancake separation. We also find that the energy of the isolated chain as a function of pancake-stack separation has a minimum, i.e., there is an optimum density of pancake stacks along a chain, and there will be an instability towards *clustering* when the total density is low. As the density of pancake stacks along the chain increases (at a fixed density of Josephson vortices), the chain will *buckle*

(Section III), and then *eject* vortices at a critical minimum separation (Section IV). More surprisingly, at very low pancake density the chain state may be replaced by a chain of tilted stacks (Section V). These results are summarized in Figs. 2 and 3, where we plot the calculated phase boundaries for three first-order transitions: clustering, buckling and tilting as well as a continuous ejection transition. Finally, in Section VI we discuss the extent to which these transitions have been observed experimentally, and consider the effect of fluctuations due to finite temperature or quenched pinning disorder.

We conclude this introduction with a note on parameters. The experiments we have referred to,[6,11,16] were performed on the extremely anisotropic cuprate $Bi_2Sr_2CaCu_2O_x$ (BiSCCO). Where we make explicit calculations we will take the following appropriate parameters $\gamma = 500$, $\lambda = 2000$ Å, and $d = 15$ Å. This gives a Josephson length (the size of the non-linear core of a Josephson vortex) of $\gamma d = 7500$ Å $\gg \lambda$.

II. STRUCTURE OF THE ISOLATED VORTEX CHAIN

Koshelev has estimated the structure of a pancake stack that crosses the center of a single Josephson vortex.[13] In the crossing configuration there is a Lorentz force on the pancakes in a direction parallel to the Josephson vortex, which must balance the attraction of each pancake to its stack. This distorts the pancake stack, with the largest displacements by the two pancakes immediately above and below the Josephson core. The distortions give an energy gain of $\Delta E_\times \approx -8.4\varepsilon_0 d(\lambda/\gamma d)^2/\ln(3.5\gamma d/\lambda)$. Here $\varepsilon_0 d = (\Phi_0/4\pi\lambda)^2 d$ is the typical energy scale for pancake interactions. This causes the pancake stack to be attracted to a stack of Josephson vortices within the crossing-lattice state. Koshelev's result uses a quadratic approximation for the pancake-to-stack attraction. Recent work[21] using the correct potential has shown that, while Koshelev's estimate for the crossing energy is close to the full result, a stable crossing configuration only exists for extreme enough anisotropy, $\gamma > \gamma_{\rm min} = 2.86\lambda/d$. In this section we include the interaction between pancakes in different stacks separated by $a_{\rm ch}$ along an isolated chain. For finite $a_{\rm ch}$ we find a further reduction of the stability limit of crossing found in Ref. 21. We also find a minimum in the energy of the chain as a function of stack separation, which leads to a clustering instability when $a_{\rm ch} \gg \lambda$.

To calculate the crossing configuration of the chain, we use the following assumptions: First, we neglect the effect of induced Josephson currents due to displacing pancakes from their stacks (reasonable for large values of $\gamma d/\lambda$ and small enough displacements $u < \gamma d$). Second, we utilize the long range of the remaining electromagnetic pancake interactions,[17] of order λ in the z-direction. There are many ($\sim \lambda/d \sim 10^2$) pancakes that contribute to the current distribution in one layer, determining the potential felt by a given pancake. We can therefore reduce this many-body optimization problem to a one-dimensional problem, considering the displacement of a row of pancakes in one layer under the potential due to the ideal chain of pancake stacks (the corrections due to the displacements in other layers is small when the number of pancakes with large displacements is much less than λ/d).

Within this scheme, the energy profile (per stack) for displacing by u_n a row of pancakes in the nth layer when there is a Josephson vortex between layers 0 and 1 crossing the chain is,

$$\Delta E_n(u_n) = -\frac{\Phi_0 d}{c} J_n^y u_n + V_{\rm em}^{\rm row}(u_n). \qquad (1)$$

The first term here comes from the Lorentz force on the pancakes due to the in-plane current density from the Josephson vortex, J_n^y, and tends to pull the pancakes away from their stacks. The form of this current will be discussed more in Section III, but the numerical value is taken from Ref. 28, e.g., the current in the $n = 1$ layer (immediately above the Josephson vortex) is $J_1^y = 2.28\varepsilon_0 c/\Phi_0\gamma d$. The second term is the attractive magnetic interaction of the pancake row with the remainder of all the stacks in the chain. Clem showed for a single pancake,[24] that this has the same interaction energy as the sum of a pancake with a full stack, $V_{\rm em}^{\rm stack}(R) = 2\varepsilon_0 d K_0(R/\lambda)$ plus a pancake with its anti-image $V_{\rm em}^{\rm pc-pair} = 2\varepsilon_0 d \ln(R/L)$, so that for the entire row we find

$$V_{\rm em}^{\rm row}(u) = 2\varepsilon_0 d\left[K_0(u/\lambda) + \ln(u/2\lambda) + \gamma_{\rm E}\right] \qquad (2)$$
$$+2\varepsilon_0 d \sum_{j\neq 0} K_0\left[\frac{j a_{\rm ch} + u}{\lambda}\right] - K_0\left(\frac{j a_{\rm ch}}{\lambda}\right) + \ln\left[\frac{j a_{\rm ch} + u}{j a_{\rm ch}}\right].$$

[Euler's constant $\gamma_{\rm E}$ is needed to fix the zero of energy to that of fully aligned stacks, c.f. the small x expansion of the modified Bessel function $K_0(x)$].

Such energy profiles for the $n = 1$ pancake row are shown in Fig. 4 for different values of $a_{\rm ch}$ with the choice of the ratio $\gamma d/\lambda = 3.75$ (a reasonable choice for BiSCCO). For dilute chains there is a stable minimum (as expected from the results of Ref. 21), which determines the optimal displacement. However, this stability disappears once the separation is below the critical value of $a_{\rm ch}^{\rm min} = 5.3\lambda$. There can be no stable isolated-chain state for densities higher than this critical value.[22] Fig. 4 also suggests that the crossing configuration is only metastable, with a lower energy at $u_1 = 0.5 a_{\rm ch}$, but this is not reliable as the simple Lorentz force argument does not hold for pancake displacements of such a large fraction of the stack-separation. For such displacements the original Josephson vortex becomes completely fragmented, and a different approach is needed. In fact, the competing state here is a "tilted chain", and in Section V we will calculate the energy of the tilted chain, to compare to the isolated chain state. (A third possibility is a soliton-like structure[23] that we will not consider here.)

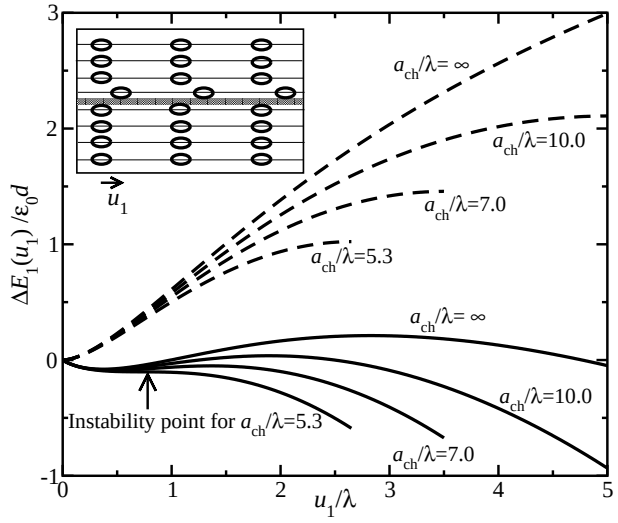

FIG. 4: Energy profiles for displacing a pancake row within a chain of pancake stacks, $V_{\rm em}^{\rm row}(u_1)$, (dashed lines) and the total energy change $\Delta E_1(u_1)$ with a Josephson vortex below the pancake row (full lines), for different values of the pancake-stack spacing $a_{\rm ch}$. Note how the metastable minimum disappears for spacings smaller than $a_{\rm ch}^{\rm min} = 5.3\lambda$. Each curve is only plotted up to $u_1 = a_{\rm ch}/2$. The fact that, for all values of $a_{\rm ch}$ the lowest energy is for large displacements, is not a physical result, as the Lorentz force argument will break down when u_1 is a significant fraction of $a_{\rm ch}$. These results are for a fixed value of $\gamma d/\lambda = 3.75$.

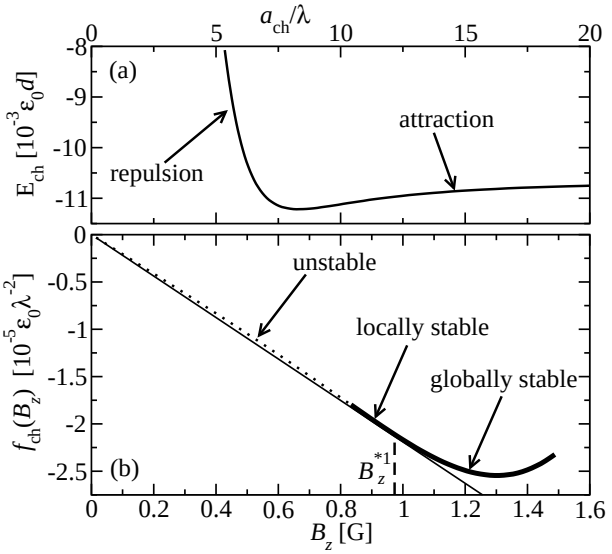

FIG. 5: (a) The energy per pancake within the isolated chain as a function of separation $a_{\rm ch}$ when $a_{{\rm J}z} = 20d$. Note the presence of a minimum energy at $a_{\rm ch} = 8.2\lambda$. (b) The same result, but expressed as the energy density $f_{\rm ch}(B_z)$ as a function of the out-of-plane flux density $B_z = \Phi_0/a_{\rm ch}a_{{\rm J}y}$. The thick line shows where the function has positive curvature, required to ensure local stability. The entire function must be convex, and so for densities less than B_z^{*1} the chain will phase separate into clusters with $a_{\rm ch} = a_{\rm ch}^{*1}$ and regions with no stacks.

The displacements of the entire stacks are shown in Fig. 1 for $a_{\rm ch} = 10\lambda$, and a Josephson-vortex separation of $a_{{\rm J}z} = 20d$ (this corresponds to $B_x = 53$ G for our parameters). All of the displacements contribute to the total crossing energy gain. We find that the crossing energy per pancake stack only lowers from $\Delta E_\times(\infty) \approx -0.21\varepsilon_0 d$ for an isolated stack to $\Delta E_\times(a_{\rm ch}^{\rm min}) \approx -0.26\varepsilon_0 d$ as the stacks reach the critical separation $a_{\rm ch}^{\rm min}$. Therefore within the region of stable crossing, there is a pinning energy to the Josephson vortex centers per unit length of pancake stack,

$$\varepsilon_{{\rm Jv-pin}} = \Delta E_\times / a_{{\rm J}z} \approx 0.2\varepsilon_0 (d/a_{{\rm J}z}), \qquad (3)$$

where the last result is with our parameters for BiSCCO.

In Fig. 5a we plot the total energy per pancake of the isolated chain $E_{\rm ch} = \frac{1}{2}\sum_{j\neq 0} V_{\rm em}^{\rm stack}(ja_{\rm ch}) + (d/a_{{\rm J}z})\Delta E_\times(a_{\rm ch})$. Note that there is a minimum at $a_{\rm ch} = 8.2\lambda$, reflecting the fact that at large separations the pancake stacks attract each other. This unusual feature has been explained by Buzdin and Baladie[26] by considering the distorted pancake stacks of Fig. 1 as the superposition of a straight stack plus a series of pancake–anti-pancake dipoles. The straight stacks give a repulsive term, but this is exponentially small for $a_{\rm ch} \gg \lambda$, while the dipoles give a weak attractive term that only falls off like $1/a_{\rm ch}^2$ (note there is some similarity to the attraction between tilted flux lines[20]). Therefore there is a net attraction at large distances, which will destabilize a homogeneous chain at very low densities.

To formally describe this instability we should consider the free energy density as a function of out-of-plane field, $f(B_z) = f_{\rm ch}(B_z) + \varepsilon_{\rm stack}B_z/\Phi_0$. Here $\varepsilon_{\rm stack}$ is the line energy of a pancake stack, $f_{\rm ch}(B_z) = E_{\rm ch}(a_{\rm ch})/a_{\rm ch}a_{{\rm J}y}d$ and $B_z = \Phi_0/a_{\rm ch}a_{{\rm J}y}$. In Fig. 5b we plot $f_{\rm ch}(B_z)$ using the same data in Fig. 5a. We also note that the thermodynamically stable phase is determined by the minimum Gibbs free energy $g(H_z) = f[B_z(H_z)] - B_z H_z/4\pi$ with $H_z = 4\pi\partial f/\partial B_z$. By a geometric construction we see that the point $B_z = B_z^{*1}$ on $f_{\rm ch}(B_z)$ where a straight line from the origin connects with the same gradient must have $g = 0$, and there is a first-order phase transition between a Meissner phase with no pancake stacks and a finite density of stacks with $a_{\rm ch} = a_{\rm ch}^{*1}$. All the points at lower density $B_z < B_z^{*1}$ have $g > 0$ and so are thermodynamically unstable. In fact, similar arguments determine that $f_{\rm ch}(B_z)$ must always be a convex function. The dotted line represents the region where the curvature of $f_{\rm ch}(B_z)$ is positive, meaning that the solution here is always unstable.

The straight line that determines B_z^{*1} is given by $f = B\delta H_{\rm c1}^z/4\pi$ where $\delta H_{\rm c1}^z$ is the change in the lower critical field due to the attraction of pancake stacks to the Josephson vortices. In Fig. 5b it is given by $\delta H_{\rm c1}^z = -2.5\cdot 10^{-3} H_{\rm c1}^z$ which is hardly measurable. In real experiments however, the geometry of the samples often makes demagnetization effects important such that the average B_z becomes fixed to the external field $H_{\rm ext}$,

rather than to H. This means that small values of B_z are accessible, and that for $B_z < B_z^{*1}$ we may expect a coexistence of $B_z = 0$ and $B_z = B_z^{*1}$ phases (c.f. the intermediate state in type-I superconductors[27]). Alternatively we could describe this mixed regime in terms of "clusters" of pancake stacks with separation $a_{\rm ch}^{*1}$. The relative proportion of space taken up by these clusters is determined by the value of B_z, but the size of individual clusters depends on the energy of the "domain wall" between the cluster of stacks and the region of no stacks, compared to the magnetic energy cost of large clusters with the wrong flux density. Also, in the experimental situation one can have different pancake densities on the different chains, so the inhomogenous state may have coexisting empty and filled chains. Our results for the critical field separating the clustered phase from the homogeneous isolated straight chains are shown in Figs. 2 and 3.

III. BUCKLING INSTABILITY WITHIN VORTEX CHAIN

It is important to realize that, while the isolated-chain state gains energy due to the Lorentz force of the Josephson vortex currents, there is an energy penalty for the pancake stacks to be close to each other. One consequence of this is a maximum density above which pancake stacks will be ejected from the chain. This critical density will be derived in the next section. Below this density, however, the chain can already react to the stack repulsion by buckling. Note that we will assume that the Josephson vortices remain straight, as in experiments they are held in place by the interactions with Josephson vortices in neighboring chains, and the chain separation is much smaller than the interaction range for Josephson vortices, $a_{Jy} \ll \gamma\lambda$. In contrast, the interactions between pancake stacks on different chains are in the dilute limit, $a_{Jy} \gg \lambda$, and so are easily displaced.

To calculate this buckling, we need to know the energy gain from a crossing event when the pancake stack is displaced away from the center of a Josephson vortex. We therefore need the full current profile of a Josephson vortex, which is a solution of the non-linear equations that arise from the London-Lawrence-Doniach model.[9,18] An accurate numerical solution for a Josephson vortex is described in Appendix B of Ref. 25. For a vortex directed along $\hat{\mathbf{x}}$ centered at $y = 0$ and between the $n = 0, 1$ layers, the current in the y direction can be written[28] (ignoring screening, i.e. $n < \lambda/d$ and $y < \lambda_c$),

$$J_n(y) = \frac{2c\varepsilon_0}{\Phi_0\gamma d} p_n(y/\gamma d), \tag{4}$$

with $p_n(\tilde{y}) = \phi_n'(\tilde{y})$ the reduced superfluid momentum, where the phase has the form,[29]

$$\phi_n(\tilde{y}) = \tan^{-1}\left[\frac{(n-\frac{1}{2})}{\tilde{y}}\right] + \frac{0.35(n-\frac{1}{2})\tilde{y}}{[(n-\frac{1}{2})^2+\tilde{y}^2+0.38]^2}$$

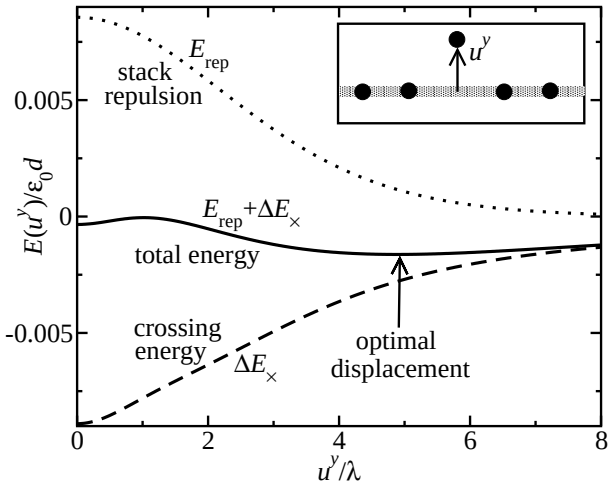

FIG. 6: The energy profile when we pull one pancake stack away a distance u^y from the isolated chain state, for $a_{\rm ch} = 5.5\lambda$, and $a_{Jz} = 25d$. The geometry is shown in the inset. The dashed line shows the energy from the crossing events on the displaced stack. The dotted line is the interaction energy of displaced stack with the other stacks on the chain. The full line is the sum of these two contributions. Note the presence of two minima, one for $u^y = 0$, and a lower minimum at $u^y = 4.9\lambda$.

$$+\frac{8.81(n-\frac{1}{2})\tilde{y}[\tilde{y}^2-(n-\frac{1}{2})^2+2.77]}{[(n-\frac{1}{2})^2+\tilde{y}^2+2.02]^4}. \tag{5}$$

When $y = 0$, this gives the results used in Section II, with $J_n(0) = (2c\varepsilon_0/\Phi_0\gamma d)C_n/|n-\frac{1}{2}|$, and $C_1 = 0.57$, $C_2 = 0.86$, $C_3 = 0.99$, and $C_n \approx 1$ for $n > 3$.

We can now recalculate the crossing energy for an arbitrary distance between a pancake stack and the center of a Josephson vortex. Within the quadratic approximation used in Refs.13 and 28 one can easily solve the crossing configuration for a single stack. Writing $\Delta E_n(u_n) = -(\Phi_0 d/c)J_n(y)u_n + \frac{1}{2}\alpha u_n^2$, where we take $\alpha = (\varepsilon_0 d/\lambda^2)\ln(\lambda/r_w)$ with r_w a short distance cut-off, we find the relaxation energy,

$$\Delta E_\times(y) = -2\left(\frac{\lambda}{\gamma d}\right)^2 \frac{1}{\ln(\lambda/r_w)} \sum_{n=-\infty}^{\infty} [p_n(y/\gamma d)]^2 . \tag{6}$$

Koshelev takes $r_w = u_1$ ($\approx 0.29\lambda^2/\gamma d$ for $y = 0$), and in Ref. 21 we have shown this to be a good approximation to the result when the full form of the pancake-stack interaction is used.

This result for the crossing energy as a function of stack displacement u^y is shown as the dashed line in Fig. 6, where there is one Josephson vortex for every 25 pancakes along a stack. As might be expected, the energy increases quadratically at small u^y. More interesting is the fact that the crossing energy vanishes only as $\Delta E_\times \approx -\lambda^2/u^{y2}$ for $u^y \gg \gamma d$ (note that an exponential suppression will occur at extremely long distances $u^y > \lambda_c$). In contrast, also shown in Fig. 6 (the dotted line) for $a_{\rm ch} = 5.5\lambda$ is the repulsive energy

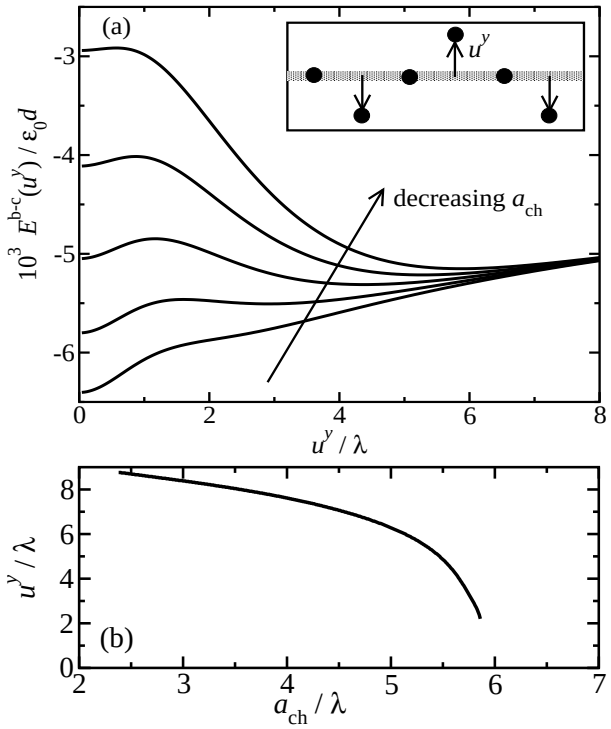

FIG. 7: (a) Energy of the buckled chain (see inset) as a function of the buckle parameter u^y, for stack separation along the chain $a_{\rm ch}/\lambda = 5.2$, 5.4, 5.6, 5.8, and 6.0. For the separation $a_{\rm ch}/\lambda = 6.0$ there is only one minimum at $u^y = 0$. For $a_{\rm ch}/\lambda = 5.8$ there is a second minimum at $u_y = 3.3\lambda$. The remaining cases have their lowest minimum at finite u^y. (b) The size of the optimum buckling distortion $u^y_{\rm opt}$ as a function of $a_{\rm ch}$.

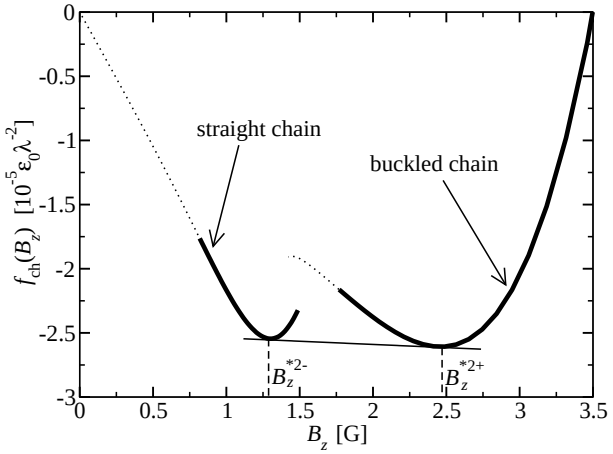

FIG. 8: Energy density of the buckled-chain state with $a_{Jz} = 20d$ as a function of out-of-plane field B_z. Also shown is the result for the straight chain from Fig. 5b. The two points joined by the straight line have the same Gibbs free energy, and those densities between these points are thermodynamically unstable towards a mixed phase of straight and buckled chains.

cost for displacing one pancake stack away from a chain, $E_{\rm rep} = \sum_{j\neq 0} V_{\rm em}^{\rm stack}\left(\sqrt{(ja_{\rm ch})^2 + u^{y2}}/\lambda\right)$. This contribution vanishes exponentially when $u^y > \sqrt{a_{\rm ch}\lambda}$, and so the total energy is always negative for large enough u^y. This gives the possibility of two minima in the total energy (see the full line in Fig. 6), and a first-order transition where the displacement jumps to a finite value as $a_{\rm ch}$ decreases. While we have started by considering displacing a single stack from the chain, it is this instability that drives a buckling of the whole chain.

To estimate the buckling transition we use a variational approach for the buckled configuration (See the inset of Fig. 7a). This configuration is only characterized by a single displacement parameter u^y, and so we can look at the energy profiles in u^y for different $a_{\rm ch}/\lambda$. First, the energy per pancake is calculated before crossing relaxations,

$$E_0^{\rm b-c}(u^y) = \frac{\varepsilon_0 d}{N}\sum_{i\neq j} K_0\left(\sqrt{(i-j)^2 a_{\rm ch}^2 + (y_i - y_j)^2}/\lambda\right) \quad (7)$$

with $y_i = 0$ for i even, and $y_i = (-1)^{(i+1)/2}u^y$ for i odd. Next we checked for the stability of crossing, as in Section II, and found that the crossing configuration becomes unstable if $a_{\rm ch} < 2.65\lambda$. Finally, to calculate the energy gain from crossing the Josephson vortices, we use the result (6) giving the total energy of the buckled chain,

$$E^{\rm b-c}(u^y) = E_0^{\rm b-c}(u^y) + \frac{d}{2a_{Jz}}[\Delta E_\times(0) + \Delta E_\times(u^y)]. \quad (8)$$

In Fig. 7a we plot this energy for $a_{\rm ch}/\lambda$ from 5.2 to 6.0, with $a_{Jz} = 25d$, showing how the minimum energy of a buckled chain crosses the energy of a straight chain as $a_{\rm ch}$ decreases. Note that the minimum for a finite u^y is quite shallow, and so we might expect large fluctuations in the extent of buckling along the chain due to random vortex pinning, which is discussed in Section VI. Also shown in Fig. 7b is the optimal displacement $u^y_{\rm opt}$ as a function of $a_{\rm ch}$, which has a smallest value of $u^y_{\rm opt} = 2.3\lambda$ at the first appearance of (meta)stable buckling at $a_{\rm ch} = 5.8\lambda$ and then increases at higher densities.

It has been shown in Section II that one should plot the energy density of the chain as a function of the out-of-plane flux density B_z, in order to determine the stable thermodynamic phases. Such a plot is shown in Fig. 8 comparing the straight and buckled chains. It shows that the isolated straight chains at $B_z = B_z^{*2-} \approx 1.3$ G has the same Gibbs free energy as the buckled-chain state at $B_z = B_z^{*2+} \approx 2.5$ G. Therefore at fields with $B_z^{*2-} < B_z < B_z^{*2+}$ the thermodynamic phase will be a coexistence of straight and buckled regions, with the relative proportion linearly dependent on B_z. Note that B_z^{*2-} is only slightly higher than B_z^{*1} so that there is only a small regime where pure isolated straight chains are the stable phase. The same procedure has been followed for a range of a_{Jz}/d, and the resulting boundaries to the mixed buckled chains are shown in Figs. 2 and 3.

IV. EJECTION OF PANCAKE STACKS FROM ISOLATED CHAIN

We now consider a simple model for the energy of the composite state where a fraction of the pancake stacks are not located on the chains. This model will show that there is a continuous phase transition between this composite state and the isolated-chain state as a function of B_z. The order parameter of this transition is the density of the dilute lattice of pancake stacks not trapped on chains. The simple model assumes that the chain spacing $a_{\mathrm{J}y}$, and the spacing between pancake stacks is much greater than the penetration depth λ. In this case we can separate the total interaction energy density of pancake stacks in the form $f_{\rm tot} = f_{\rm ch}(\nu_{\rm ch}) + f_{\rm dil}(\nu_{\rm dil})$, where $\nu_{\rm ch}$ and $\nu_{\rm dil}$ are the (2D) densities of pancake stacks on and off the chains respectively, and the total density is $\nu_{\rm ch} + \nu_{\rm dil} = \nu_{\rm tot} = B_z/\Phi_0$. The separation of pancakes along the chain is $a_{\rm ch} = 1/a_{\mathrm{J}y}\nu_{\rm ch}$. The chain energy $f_{\rm ch}(\nu_{\rm ch})$ is to be calculated as in Sections II and III for straight and buckled chains respectively. We will see that the phase transition to the composite state occurs when there is a minimum in $f_{\rm ch}(\nu_{\rm ch})$, and so near this transition we will expand,

$$f_{\rm ch}(\nu_{\rm ch}) = \epsilon' \lambda^2 (\nu_{\rm ch} - \nu_{\rm ch}^{\rm c})^2. \tag{9}$$

The density of pancake stacks not on a chain is small near the transition, so that the interaction energy density is simply (using the limit $K_0(x) \approx \sqrt{\pi/2x}e^{-x}$ and only including nearest neighbors),

$$f_{\rm dil}(\nu_{\rm dil}) = 3\varepsilon_0\sqrt{2\pi\lambda}\,\nu_{\rm dil}^{-5/4} e^{-1/\lambda\nu_{\rm dil}^{1/2}}. \tag{10}$$

Note that in the small $\nu_{\rm dil}$ limit, all terms in a power series expansion of $f_{\rm dil}(\nu_{\rm dil})$ are zero, i.e. the function is extremely flat. For this reason the critical total density at the transition is only determined by the minimum in $f_{\rm ch}(\nu_{\rm ch})$ at $\nu_{\rm ch}^{\rm c}$. For $\nu_{\rm tot} < \nu_{\rm ch}^{\rm c}$, all of the pancake stacks are on chains. At densities just above $\nu_{\rm ch}^{\rm c}$ the energy is minimized with a dilute off-chain density,

$$\nu_{\rm dil} = \delta\nu_{\rm tot} - \frac{3\sqrt{2\pi}}{4}\frac{\varepsilon_0}{\varepsilon'}\frac{1}{\lambda^{5/2}\delta\nu_{\rm tot}^{1/4}} e^{-1/\lambda\delta\nu_{\rm tot}^{1/2}}. \tag{11}$$

The second term is extremely small for the fields we are interested in $B_z \ll \Phi_0/\lambda^2$, so that we can say in the composite state at $\nu_{\rm tot} > \nu_{\rm ch}^{\rm c}$ there is a fixed density on the chains $\nu_{\rm ch} = \nu_{\rm ch}^{\rm c}$ and the remaining density is $\nu_{\rm dil} = \nu_{\rm tot} - \nu_{\rm ch}^{\rm c}$. The phase boundary $\nu_{\rm ch}^{\rm c}$ between the composite state and the isolated-chain state is calculated from the minimum of $f_{\rm ch}$. In Figs. 2 and 3 this boundary is plotted, but is not distinguishable by eye from the transition between mixed buckled and pure buckled chain. Therefore the pure buckled chain has a very narrow range of existence. It is worth stating that an ejection transition has been observed experimentally[16] with results that seem to be consistent with the above, although a quantitative analysis of the transition has not yet been published.

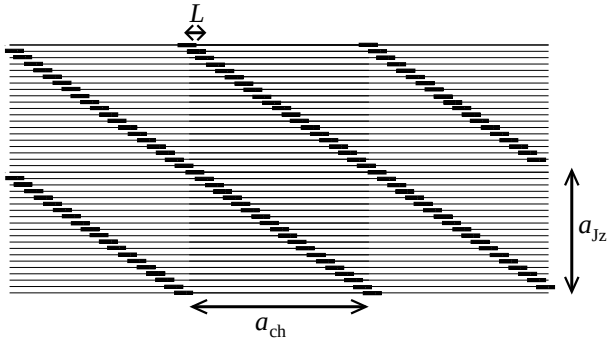

FIG. 9: Configuration of the tilted chain, where pancakes in a stack are displaced from layer to layer by $L = a_{\rm ch}/a_{\mathrm{J}z}$.

V. CROSSING-TO-TILTED TRANSITION WITHIN ISOLATED CHAINS

In this section we calculate the energy of a chain of tilted vortices, and compare to the chain of crossing vortices. The tilted chain is an alternative configuration to the crossed chain with the same density of pancake and Josephson vortices (see Fig. 9) where the tilt angle is determined by $\tan\theta = L/d = a_{\rm ch}/a_{\mathrm{J}z}$. These tilted stacks have an increased energy of pancake interactions but there may be an energy gain from replacing fully developed Josephson vortices with many short Josephson segments of length $L < \gamma d$. To calculate the energy of the tilted chain, we use the linear approximation of the London-Lawrence-Doniach model,[9,25] where we ignore the non-linear effects from regions with large phase differences across neighboring layers. This approximation is justified as long as the length L is much smaller than the Josephson length γd and the pancake separation $a_{\rm ch}$. Note that the condition $L < \gamma d$ corresponds to $B_x/B_z < \gamma$, which is the case we are interested in. The energy due to pancake interactions in the linear approximation is,

$$E_{\rm pc}^{\rm tilt} = \frac{1}{8\pi}\int \frac{d^2k}{(2\pi)^2}\frac{dq}{2\pi}\frac{\left[1+(\gamma\lambda)^2(k^2+\tilde{q}^2)\right]\ |S_z|^2}{\left[1+\lambda^2(k^2+\tilde{q}^2)\right]\left[1+(\gamma\lambda)^2k^2+\lambda^2\tilde{q}^2\right]} \tag{12}$$

with $S_z(\mathbf{k},q) = \Phi_0 d\sum_{j,n} e^{-iqnd}e^{-ik_x(ja_{\rm ch}+nL)}$ and $\tilde{q}^2 = (2/d)^2\sin^2(qd/2)$. The integral should be cut off due to the pancake cores at $k > \pi/\xi_{\rm ab}$ and due to the layered structure at $q > \pi/d$. Similarly, the Josephson segments interact with an energy contribution,

$$E_{\rm Jv}^{\rm tilt} = \frac{1}{8\pi}\int \frac{d^2k}{(2\pi)^2}\frac{dq}{2\pi}\frac{|S_x|^2}{\left[1+(\gamma\lambda)^2k^2+\lambda^2\tilde{q}^2\right]} \tag{13}$$

with $S_x = \frac{2\Phi_0}{k_x}\sin\left(\frac{k_xL}{2}\right)\sum_{j,n} e^{-iq(n+\frac{1}{2})d}e^{-ik_x[ja_{\rm ch}+(n+\frac{1}{2})L]}$.

The integrals can all be done exactly, leaving a sum over the values of $k_x = 2\pi m/a_{\rm ch}$. We have evaluated these sums numerically to find the energy of the tilted chain. This is shown for $a_{\mathrm{J}z} = 25d$ as the dotted line in Fig. 10. Also shown as the full line is the energy per

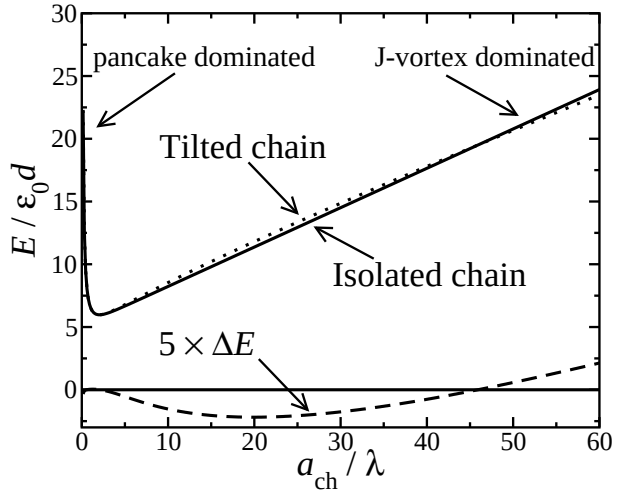

FIG. 10: Energy per pancake of the tilted chain (dotted line) and the chain of straight pancake stacks crossing Josephson vortices, for $a_{Jz} = 25d$, plotted against the pancake separation a_{ch}/λ. Also shown (dashed line) is the difference of the two energies, which crosses zero at $a_{ch} = 45\lambda$.

pancake of the crossing chain with the same density of pancakes and Josephson vortices, $E_{cross} = E_{ch} + E_{Jv}^{cross}$, where E_{ch} is defined in Section II and

$$E_{Jv}^{cross} = \frac{\varepsilon_0 d}{\gamma}\frac{a_{ch}}{a_{Jz}}\left[1.55 + \ln\left(\frac{\lambda}{d}\right) + \sum_{j\neq 0} K_0\left(\frac{j a_{Jz}}{\lambda}\right)\right]. \quad (14)$$

The tilted chain has a lower energy from Josephson vortex contributions (dominant at low density) but a higher energy from pancake vortex contributions (dominant at high density), and there is a first-order transition between the isolated chain of straight stacks and the chain of tilted stacks. In fig. 10 it is shown that for $a_{ch} < 45\lambda$ (higher density) the preferred state is the crossing chain, while for $a_{ch} > 45\lambda$ (lower density), the lowest energy is for the tilted chain. Note that Savelev et al.,[30] also find a "reentrant" transition back to a tilted lattice for fields close to the ab-plane, when $\lambda > \gamma d$.

A strict treatment should follow Sections II and III and consider the points of the same Gibbs free energy density. This is not possible within our level of treatment, however, as we would need accurate results at very low $B_z < B_x/\gamma$ where non-linear effects in the tilted chain are important. Here, we can only show that there must be a low-density transition to the tilted chain, but we cannot plot the coexistence boundaries. Even so, we plot the line where the energies cross in Figs. 2 and 3 separating the clustered chain from a tilted chain phase. In real experiments there is a finite 2D density of Josephson vortices, which cannot be considered isolated in the sense of the pancake vortex chains (the interaction range λ_c is greater than the chain spacing a_{Jy}). Therefore a full calculation of the 3D tilted lattice requires a minimization over the aspect ratio, which we leave for a future work.

VI. DISCUSSION

We now discuss the extent to which these transitions have been observed experimentally. In the recent scanning Hall probe experiments of Grigorenko et al.,[16] there does seem to be a sharp transition as a function of B_z between a composite state of chains with a dilute lattice and the isolated chain state, as derived in Section IV. At lower fields there is some evidence for buckling and clustering (Sections II and III) although the influence of pinning disorder may be contributing to this. Finally, Grigorenko et al. report a strange transition at very low B_z where the chains are replaced by faint, homogeneous "stripes" of flux. These stripes would be consistent with the flux distribution from a tilted chain, and it is likely that a transition from the isolated-chain state to a tilted-chain state (as found in Section V) takes place. Experimentally, a large jump in B_z (i.e. in the pancake density) is seen at the transition to tilted chains; unfortunately we were not able to calculate the jump in this paper, as it requires an accurate treatment of non-linear effects in the small B_z limit. Other experimental features are that the tilted chains are much straighter than the crossing chains, and less pinned. This is consistent with the fact that the tilted chains are really part of a 3D line lattice with stronger interactions that dominate over pinning disorder, whereas in the crossing case the pancake stacks are in the extreme dilute limit, and therefore easily pinned in random low-energy sites.

Finally, we briefly discuss the effect of fluctuations. The calculations in this paper have found the lowest-energy vortex configurations of the chains. In reality there will be distortions of these states due to thermal fluctuations and random pinning to inhomogeneities in the underlying crystal. It is well established that thermal fluctuations can lead to a melting of the vortex crystal.[1] A melting transition to completely decoupled layers is studied for $B_x = 0$ in Ref. 31, involving short-wavelength fluctuations of pancake stacks with $k_z > \pi/\lambda$. While there will be some modification in the presence of Josephson vortices in tilted fields, in the low out-of-plane fields studied here, $B_z \ll \Phi_0/\lambda^2$, this melting will take place at a high temperature, close to the Berezinskii-Kosterlitz-Thouless transition[32] at $T_{BKT} = \varepsilon_0 d/2$. If we consider long wavelength fluctuations, $k_z \to 0$, then we may expect some kind of melting of the chain at very low fields due to the exponentially small interaction of pancake stacks. However, the mechanism of such a transition must be different from the "entanglement" proposed in the original derivation of low-field vortex lattice melting by Nelson.[33] Considering the nature of the crystalline order of the isolated vortex chain, we should recognize the two-dimensional nature of this state. A simple consequence is that thermal fluctuations at long wavelength will lead to a quasi-long-range ordered state. It may then be possible to have a 2D continuous melting transition via the unbinding of dislocations. However, a dislocation for this system of stacks corresponds to a stack that termi-

nates in the middle of the chain, and this should cost an energy linear in the system size, rather than the usual logarithmic energy of a dislocation. This will suppress a dislocation unbinding transition.

In the experiments of Grigorenko et al. the pinning disorder seems to be more important in disturbing the chain states than thermal fluctuations. The fact that the pancake stacks are observed in fixed positions is due to pinning (otherwise thermal fluctuations would smear out the average density in the chain state), and this also tends to disorder the chains. On general grounds we expect pinning-induced wandering of the pancake stacks within the chains so that there is only a short range order. There will also be significant transverse displacements, and the buckling effect should be enhanced by disorder.

It is a pleasure to thank Simon Bending and Sasha Grigorenko for enthusiastically introducing me to the world of chains and crossing lattices, as well as Dima Geshkenbein for useful discussions and Alex Koshelev for demonstrating how to calculate the currents near a Josephson vortex. The author is supported by an EPSRC Advanced Fellowship AF/99/0725. Work at the ETH-Zürich was financially supported by the Swiss National Foundation.

[1] A comprehensive review is G. Blatter *et al.*, Rev. Mod. Phys. **66**, 1125 (1994).
[2] E. Zeldov *et al.*, Nature **375**, 373 (1995).
[3] C. J. van der Beek *et al.*, Phys. Rev. Lett. **84**, 4196 (2000).
[4] J. Mirkovic *et al.*, Phys. Rev. Lett. **86**, 886 (2001).
[5] S. Ooi *et al.*, Phys. Rev. B **63**, 020501 (2000).
[6] C. A. Bolle *et al.*, Phys. Rev. Lett. **66**, 112 (1991).
[7] D. A. Huse, Phys. Rev. B **46**, 8621 (1992).
[8] S. Theodorakis, Phys. Rev. B **42**, 10172 (1990).
[9] L. N. Bulaevskii, M. Ledvij, and V. G. Kogan, Phys. Rev. B **46**, 366 (1992).
[10] L. J. Campbell, M. M. Doria, and V. G. Kogan, Phys. Rev. B **38**, 2439 (1988).
[11] I. V. Grigorieva *et al.*, Phys. Rev. B **51**, 3765 (1995).
[12] M. Benkraouda and M. Ledvij, Phys. Rev. B **51**, 6123 (1995).
[13] A. E. Koshelev, Phys. Rev. Lett. **83**, 187 (1999).
[14] B. Schmidt *et al.*, Phys. Rev. B **55**, R8705 (1997).
[15] S. Ooi *et al.*, Phys. Rev. Lett. **82**, 4308 (1999).
[16] A. Grigorenko *et al.*, Nature **414** 728 (2001).
[17] S.N. Artemenko and A.N. Kruglov, Phys. Lett. A **143**, 485 (1990); M.V. Feigelman, V.B. Geshkenbein and A.I. Larkin, Physica C **167**, 177 (1990); A. Buzdin and D. Feinberg, J. Phys. (France) **51**, 1971 (1990).
[18] J. R. Clem and M. W. Coffey, Phys. Rev. B **42**, 6209 (1990).
[19] G. Blatter, V.B. Geshkenbein and A.I. Larkin, Phys. Rev. Lett. **68**, 875 (1992).
[20] A. M. Grishin, A. Y. Martynovich, and S. V. Yampolskii, Sov. Phys. JETP **70**, 1089 (1990); A. I. Buzdin and A. Y. Simonov, JETP Lett. **51**, 191 (1990).
[21] M. J. W. Dodgson, to appear in Physica C.
[22] More accurately, the critical value $a_{\rm ch}^{\rm min}$ may be slightly smaller if relaxation of the Josephson-vortex in-plane current is included (A.E. Koshelev, private communication).
[23] A. E. Koshelev, private communication.
[24] J.R. Clem, Phys. Rev. B **43**, 7837 (1991).
[25] A.E. Koshelev, Phys. Rev. B **48**, 1180 (1993).
[26] A. Buzdin and I. Baladie, cond-mat/0110339.
[27] L. D. Landau and E. M. Lifshitz, *Electrodynamics of Continuous Media*, (Pergamon Press, Oxford 1960).
[28] A. E. Koshelev, unpublished.
[29] A. E. Koshelev, Phys. Rev. B **62**, R3616 (2000).
[30] S. E. Savelev, J. Mirkovic, and K. Kadowaki, Phys. Rev. B **64** 094521 (2001).
[31] M.J.W. Dodgson *et al.* Phys. Rev. Lett. **83**, 5358 (1999); Phys. Rev. Lett. **84**, 2698 (2000); Physica B **280**, 220 (2000).
[32] V.L. Berezinskii, Sov. Phys. JETP **32**, 493 (1971); J.M. Kosterlitz and D.J. Thouless, J. Phys. C **6**, 1181 (1973).
[33] D. R. Nelson, Phys. Rev. Lett. **60**, 1973 (1988).